

Using Conformal Maps to Explore the Potential of Wire Grids

Tudor Dimofte

Joseph Henry Laboratories, Princeton University, Princeton, NJ 08544

(July 28, 2003)

Abstract

This paper calculates and explores the electric potentials of wire grids¹ sandwiched between conducting planes, using the technique of conformal mapping. The initial inspiration for the problem arose from some questions about the potential of wire grids placed in drift chamber particle detectors[B, BR, M]. What voltage should we apply to a certain grid to capture drifting electrons on it? What voltage should we apply to let the electrons pass through? Herein, we first describe the general technique of using conformal maps to find electric potentials. Then, we find the potentials of some generalized grids, and describe the accuracy of approximations we might use for infinite grids. Finally, we apply our methods to attempt to model the grids of a real drift chamber.

Contents

1	Harmonic and holomorphic functions	1
1.1	The utility of conformal maps	1
2	The potential of a charged wire between two grounded conducting planes	2
3	A finite wire grid between between two non-grounded conducting planes	4
3.1	Rescaling	5
3.2	Explicit form	5
4	Infinite grids	6
4.1	Condition 1	7
4.2	Condition 2	10
4.3	Evaluation	12
4.4	Remarks	13
5	Multiple realistic grids and boundary conditions: an attempt at modelling	15
5.1	$K = 1$, one grid	16
5.2	$K > 1$, multiple grids	17
5.3	An example	17
5.4	Some brief comments on error	20
5.5	The y -derivative	22

¹“Grid” here refers to a series of parallel wires lying in a given plane. Perhaps “grill” may have been a better word for this; but the terminology seems to be quite standard for particle detectors. *Two* grills of wires, overlaid and crossing at right angles, are referred to as a “mesh”.

1 Harmonic and holomorphic functions

It is well-known² that the real and imaginary parts of a holomorphic (analytic) function³ $f(z)$ are harmonic. Indeed, writing $f(z) = u(z) + i v(z)$, with $z = x + iy$, f is holomorphic if and only if the Cauchy-Riemann equations,

$$\begin{aligned}\frac{\partial u}{\partial x} &= \frac{\partial v}{\partial y} \\ \frac{\partial u}{\partial y} &= -\frac{\partial v}{\partial x}\end{aligned}\tag{2}$$

are satisfied. But then we get

$$\begin{aligned}\Delta u &= \frac{\partial^2 u}{\partial x^2} + \frac{\partial^2 u}{\partial y^2} \\ &= \frac{\partial}{\partial x} \left(\frac{\partial v}{\partial y} \right) + \frac{\partial}{\partial y} \left(-\frac{\partial v}{\partial x} \right).\end{aligned}$$

And, assuming that u and v are twice continuously differentiable,⁴ we have

$$\Delta u = \frac{\partial^2 v}{\partial x \partial y} - \frac{\partial^2 v}{\partial x \partial y} = 0.\tag{3}$$

A corresponding result holds for v .

Now consider a (real-valued) harmonic function $h(z)$ on the complex plane, $\Delta h = 0$, and a holomorphic function $f(z)$. It can be shown that it is possible to construct a real-valued function $j(z)$ such that $h + ij$ is holomorphic; *i.e.* there exists a holomorphic function $g(z)$ such that $h = \Re(g)$. If we take this g and compose it with our initial holomorphic function f , we obtain another holomorphic function $g \circ f$. But, we know then that $\Re(g \circ f) = h \circ f$ must be harmonic. In other words, a harmonic function composed with a holomorphic function is again harmonic.

1.1 The utility of conformal maps

The above observation characterizes the use of holomorphic bijections (*i.e.* conformal maps) in finding harmonic functions. For suppose we are seeking a harmonic function u in a two-dimensional region Ω which satisfies certain boundary conditions on $\partial\Omega$, say $u|_{\partial\Omega} = U$. If $f : \Omega \rightarrow \Omega'$ is conformal, and $h(z)$ is harmonic in Ω' , then $h \circ f(z)$ will be harmonic in Ω . If in addition h is such that $h|_{f(\partial\Omega)} = U$, then $h \circ f$ will also satisfy the needed boundary conditions. So $u = h \circ f$ is our harmonic function in Ω .

²Many of the “facts” stated here are taken from [SS], an excellent source on complex analysis.

³A complex-valued function is holomorphic if the derivative

$$\lim_{h \rightarrow 0} \frac{f(z+h) - f(z)}{h}\tag{1}$$

exists for all complex h . This is equivalent to f being analytic, *i.e.* expressible as a convergent Taylor series.

⁴This does follow from the fact that f is holomorphic, thus infinitely differentiable.

This technique is mainly useful when we are dealing with a complicated region Ω which can be conformally mapped to a much simpler region Ω' . Granted, the Riemann Mapping Theorem guarantees that *any* two regions (with the same connectivity) may be conformally mapped to one another. But generally we are only interested in maps that take simpler, explicit forms, so that we may actually carry out calculations with them.

Also, note that this technique only works in two dimensions. If we want to use conformal maps to find an electric potential, we can only work with three-dimensional regions which are translationally invariant along some axis (cylindrical regions).

2 The potential of a charged wire between two grounded conducting planes

We will now use conformal maps to try to find the potential of a grid of infinitely thin wires sandwiched between two infinite conducting planes. We begin with a single wire, as in Fig. 1, and then use superposition to add more. The two parallel planes are a distance b apart, and the wire is a distance d above the bottom plane. We assume the wire carries charge λ per unit length, and (for now) that the two planes are both grounded. On the complex plane, we can place the bottom plane on the x axis, the wire at the point id , and the top plane on the line $y = \Im(z) = b$.

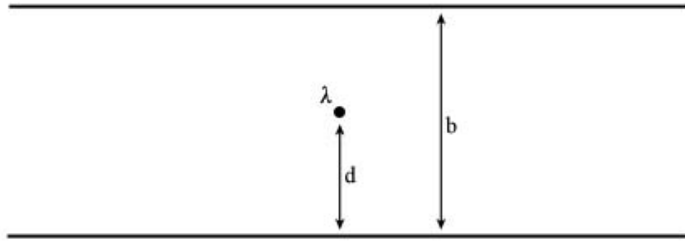


Figure 1: One wire between two conducting planes.

We would like to conformally map the infinite region between the planes to a finite, more manageable, one. We begin with the map $z \mapsto \frac{\pi z}{b}$, which scales the strip to have thickness π . Then, we apply $z \mapsto e^z$. Since $e^z = e^x e^{iy}$, the radius of image points will range between $e^{-\infty} = 0$ and $e^{\infty} = \infty$ while their angle will range between 0 and π , the thickness of the strip. So, this maps the strip to the upper half plane, taking the top plate to the positive x axis and the bottom plate to the negative x axis. Finally, we use $z \mapsto \frac{z-i}{z+i}$. Notice that,

$$\left| \frac{z-i}{z+i} \right| = \frac{|z-i|}{|z-(-i)|} \leq 1$$

for any point z in the upper half plane, so this map takes the upper half plane into the unit disk. For points on the x axis, we have $|z-i| = |z-(-i)|$; so the x axis is mapped to

the unit circle. Indeed, this is a conformal map from the upper half plane to the entire unit disk.⁵ Composing these three maps we obtain,

$$f(z) = \frac{e^{\frac{\pi z}{b}} - i}{e^{\frac{\pi z}{b}} + i}, \quad (4)$$

a conformal map that takes our strip to the unit disk, and the top and bottom plates to the unit circle.

What about our wire? Well, the wire is taken to the point $f(id)$ inside the disk. The potential of a charged wire in free space is,

$$V_f(r) = -2\lambda \log r \quad (5)$$

(in Gaussian units), where r is the perpendicular distance from the wire. If the wire is right in the center of a grounded conducting cylinder of radius R , then we may subtract a constant from V_f to force the potential to be 0 on the cylinder,

$$V_s(r) = -2\lambda(\log r - \log R) = 2\lambda \log \left(\frac{R}{r} \right). \quad (6)$$

(Notice that can look at this in complex coordinates with the wire at the origin of the complex plane and $r = |z|$.) If the wire is at an arbitrary point $\zeta = \rho e^{i\phi}$ inside a conducting cylinder of radius R then we may use the method of images to find its potential. Placing an image wire of charge $-\lambda$ at $\zeta' = \frac{R^2}{\rho} e^{i\phi} = R^2 \bar{\zeta}^{-1}$ we find that,

$$\begin{aligned} V_a(z; \zeta) &= -2\lambda \log |z - \zeta| - (-2\lambda) \log |z - R^2 \bar{\zeta}^{-1}| + C \\ &= -2\lambda \log \left| \frac{z - \zeta}{z - R^2 \bar{\zeta}^{-1}} \right| + C \\ &= -2\lambda \log \left[\left(\frac{z - \zeta}{z - R^2 \bar{\zeta}^{-1}} \right) \overline{\left(\frac{z - \zeta}{z - R^2 \bar{\zeta}^{-1}} \right)} \right]^{\frac{1}{2}} + C \\ &= -\lambda \log \left[\left(\frac{z - \zeta}{z - R^2 \bar{\zeta}^{-1}} \right) \left(\frac{\bar{z} - \bar{\zeta}}{\bar{z} - R^2 \zeta^{-1}} \right) \right] + C, \end{aligned} \quad (7)$$

where C is chosen so that $V_a(Re^{i\theta}; \zeta) = 0$. To actually find C , write $\zeta = \rho e^{i\phi}$. Then,

$$\begin{aligned} \left(\frac{z - \zeta}{z - R^2 \bar{\zeta}^{-1}} \right) \left(\frac{\bar{z} - \bar{\zeta}}{\bar{z} - R^2 \zeta^{-1}} \right) &= \frac{|z|^2 + |\zeta|^2 - 2\Re[\bar{z}\zeta]}{|z|^2 + R^4|\zeta|^{-2} - 2R^2\Re(z/\zeta)} \\ &= \frac{R^2 + \rho^2 - 2\Re(Re^{-i\theta} \rho e^{i\phi})}{R^2 + R^4 \rho^{-2} - 2R^2\Re(Re^{i\theta}/(\rho e^{i\phi}))} \\ &= \frac{\rho^2}{R^2} \left(\frac{R^2 + \rho^2 - 2R\rho \cos(\theta - \phi)}{\rho^2 + R^2 - 2R\rho \cos(\theta - \phi)} \right) \\ &= \frac{\rho^2}{R^2}. \end{aligned} \quad (8)$$

⁵To actually prove this fact (that the map is a bijection), we could come up with the inverse function, which takes the disk into the upper half plane.

So, $C = \lambda \log(\rho^2/R^2) = \lambda \log(|\zeta|^2/R^2)$ and the full expression may be written as,

$$\begin{aligned} V_a(z; \zeta) &= -\lambda \log \left[\frac{R^2}{|\zeta|^2} \left(\frac{z - \zeta}{z - R^2 \bar{\zeta}^{-1}} \right) \left(\frac{\bar{z} - \bar{\zeta}}{\bar{z} - R^2 \zeta^{-1}} \right) \right] \\ &= -\lambda \log \left[\left(\frac{z - \zeta}{z \bar{\zeta} - R^2} \right) \left(\frac{\bar{z} - \bar{\zeta}}{\bar{z} \zeta - R^2} \right) \right]. \end{aligned} \quad (9)$$

Note that this final form does reduce to $V_s(z)$ when $\zeta = 0$.

This formula gives us an expression for the potential of a charged wire inside a grounded conducting cylinder of radius R ; it of course is harmonic. So if we use f to map our original strip (along with the wire) to the unit disk and then use V_a with $R = 1$ to give us the potential *there*, we should get an expression for the potential in the strip,

$$V(z; \zeta) = V_a(f(z); f(\zeta)), \quad (10)$$

where ζ is the (complex) coordinate of the wire in the strip (in the case of the single wire, $\zeta = id$). By our construction of V_a and the mapping properties of f we see that this satisfies both the boundary condition at the wire and the condition that $V = 0$ on the grounded conducting planes. Although the complete formula, obtained by combining Eqs. 4 and 9, is rather complicated, it gives an explicit analytic expression for the potential.

3 A finite wire grid between two non-grounded conducting planes

We now wish to extend our analysis to the case where 1) there is more than one wire between the planes, and 2) the planes themselves are held at a potential difference. Suppose we have an evenly spaced grid of finite wires, as shown in Fig. 2. The distance (pitch) between two wires is a ; they are a distance d above the bottom plate, and the total plate separation is b . Let's assume we have $2N + 1$ wires, an odd number. Then, we may place a wire at id , two more at $\pm a + id$, and so on, so that the last two wires are at $\pm aN + id$. If the planes are grounded, the potential of such a configuration is given by superposition of the potentials of each individual wire,

$$V_g(z; N, a, b, d) = V(z; id) + \sum_{n=1}^N [V(z; an + id) + V(z; -an + id)]. \quad (11)$$

Note that the dependence on b is implicitly contained in f , Eq. (4) (perhaps we should have written $f(z; b)$).

We could of course also write down the potential of more than one grid between the two planes,

$$\begin{aligned} V_{Kg}(z; N_1, a_1, b_1, d_1, \dots, N_K, a_K, b_K, d_K) \\ = \sum_{k=1}^K \left[V(z; id_k) + \sum_{n=1}^{N_k} [V(z; a_k n + id_k) + V(z; -a_k n + id_k)] \right]. \end{aligned} \quad (12)$$

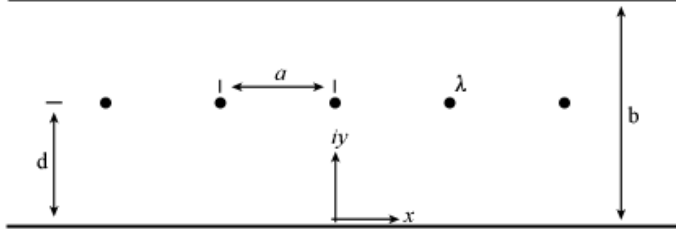


Figure 2: A wire grid between two conducting planes.

Or, if we want an infinite grid(s), we may let $N \rightarrow \infty$. Unfortunately, the resulting series does not seem to be explicitly summable.

If the planes are not both grounded but held at a potential difference \mathcal{V} we may simply add a linear potential to Eq. (11) or Eq. (12). Setting (say) the bottom plane at $V = 0$ and the top at $V = \mathcal{V}$, we obtain (instead of Eq. (11)),

$$V_g(z; N, a, b, d, \mathcal{V}) = V(z; id) + \sum_{n=1}^N [V(z; an + id) + V(z; -an + id)] + \Im(z) \frac{\mathcal{V}}{b}. \quad (13)$$

3.1 Rescaling

We might consider a certain simplification. We have been using three parameters to describe our grid geometry (a , b , and d), when in fact we really need only two. If all our grids have pitch a then we may rescale our strip via $z \mapsto z/a$ so that the pitch is always unity. In these rescaled coordinates, our potential for one grid is then,

$$V_g(z; N, b, d, \mathcal{V}) = V(z; id) + \sum_{n=1}^N [V(z; n + id) + V(z; -n + id)] + \Im(z) \frac{\mathcal{V}}{b}, \quad (14)$$

noting of course that we have also taken $b \mapsto b/a$ and $d \mapsto d/a$.

3.2 Explicit form

Before moving on, a few final calculation might prove useful (at least for computational purposes). We begin by noting that if $\zeta = n + id$ then $-n + id = -\bar{\zeta}$. Moreover,

$$f(-\bar{\zeta}) = \frac{e^{-\frac{\pi\bar{\zeta}}{b}} - i}{e^{-\frac{\pi\bar{\zeta}}{b}} + i} = \overline{\left(\frac{e^{-\frac{\pi\zeta}{b}} + i}{e^{-\frac{\pi\zeta}{b}} - i} \right)} = \overline{\left(\frac{e^{\frac{\pi\zeta}{b}} - i}{-e^{\frac{\pi\zeta}{b}} - i} \right)} = -\overline{f(\zeta)}. \quad (15)$$

So we may rewrite Eq. (14) as,

$$V_g(z; N, b, d, \mathcal{V}) = V_a(f(z); f(id)) + \sum_{n=1}^N [V_a(f(z); f(n + id)) + V_a(f(z); -\overline{f(n + id)})] + \Im(z) \frac{\mathcal{V}}{b}, \quad (16)$$

Now, adding $V_a(z; \zeta) + V_a(z; -\bar{\zeta})$ we are effectively multiplying the terms inside the logarithm. From Eq. (9) with $R = 1$, we get,

$$V_a(z; \zeta) + V_a(z; -\bar{\zeta}) = -\lambda \log \left[\left(\frac{z - \zeta}{z\bar{\zeta} - 1} \right) \left(\frac{\bar{z} - \bar{\zeta}}{\bar{z}\zeta - 1} \right) \left(\frac{z + \bar{\zeta}}{z\zeta + 1} \right) \left(\frac{\bar{z} + \zeta}{\bar{z}\bar{\zeta} + 1} \right) \right], \quad (17)$$

and the term inside the sum of Eq. (16) may be written this way, with $z \mapsto f(z)$, $\zeta \mapsto f(n + id)$. Unfortunately, this expression does not seem to yield to farther simplification.

We may, however, put in the explicit values of $f(z)$ and $f(n + id)$. After some largely uninteresting algebra we may find that,

$$V_a(f(z), f(id)) = \lambda \log \left[\frac{(e^{\frac{\pi z}{b}} - e^{-\frac{i\pi d}{b}})(e^{\frac{\pi \bar{z}}{b}} - e^{\frac{i\pi d}{b}})}{(e^{\frac{\pi z}{b}} - e^{\frac{i\pi d}{b}})(e^{\frac{\pi \bar{z}}{b}} - e^{-\frac{i\pi d}{b}})} \right] \quad (18)$$

and,

$$V_a(f(z); f(\zeta)) + V_a(f(z); -\overline{f(\zeta)}) = \lambda \log \left[\frac{(e^{\frac{\pi z}{b}} - e^{\frac{\pi \zeta}{b}})(e^{\frac{\pi z}{b}} - e^{-\frac{\pi \zeta}{b}})(e^{\frac{\pi \bar{z}}{b}} - e^{-\frac{\pi \bar{\zeta}}{b}})(e^{\frac{\pi \bar{z}}{b}} - e^{\frac{\pi \zeta}{b}})}{(e^{\frac{\pi z}{b}} - e^{\frac{\pi \zeta}{b}})(e^{\frac{\pi z}{b}} - e^{-\frac{\pi \zeta}{b}})(e^{\frac{\pi \bar{z}}{b}} - e^{-\frac{\pi \zeta}{b}})(e^{\frac{\pi \bar{z}}{b}} - e^{\frac{\pi \bar{\zeta}}{b}})} \right]. \quad (19)$$

Then,⁶

$$\begin{aligned} V_g(z; N, b, d, \mathcal{V}, \lambda) &= \lambda \log \left[\frac{(e^{\frac{\pi z}{b}} - e^{-\frac{i\pi d}{b}})(e^{\frac{\pi \bar{z}}{b}} - e^{\frac{i\pi d}{b}})}{(e^{\frac{\pi z}{b}} - e^{\frac{i\pi d}{b}})(e^{\frac{\pi \bar{z}}{b}} - e^{-\frac{i\pi d}{b}})} \right] \\ &+ \lambda \sum_{n=1}^N \log \left[\frac{(e^{\frac{\pi z}{b}} - e^{\frac{\pi(n-id)}{b}})(e^{\frac{\pi z}{b}} - e^{-\frac{\pi(n+id)}{b}})(e^{\frac{\pi \bar{z}}{b}} - e^{-\frac{\pi(n-id)}{b}})(e^{\frac{\pi \bar{z}}{b}} - e^{\frac{\pi(n+id)}{b}})}{(e^{\frac{\pi z}{b}} - e^{\frac{\pi(n+id)}{b}})(e^{\frac{\pi z}{b}} - e^{-\frac{\pi(n-id)}{b}})(e^{\frac{\pi \bar{z}}{b}} - e^{-\frac{\pi(n+id)}{b}})(e^{\frac{\pi \bar{z}}{b}} - e^{\frac{\pi(n-id)}{b}})} \right] \\ &+ \Im(z) \frac{\mathcal{V}}{b} \quad (20) \\ &= \lambda \log \left[\frac{(e^{\frac{\pi z}{b}} - e^{-\frac{i\pi d}{b}})(e^{\frac{\pi \bar{z}}{b}} - e^{\frac{i\pi d}{b}})}{(e^{\frac{\pi z}{b}} - e^{\frac{i\pi d}{b}})(e^{\frac{\pi \bar{z}}{b}} - e^{-\frac{i\pi d}{b}})} \right] \\ &\times \prod_{n=1}^N \frac{(e^{\frac{\pi z}{b}} - e^{\frac{\pi(n-id)}{b}})(e^{\frac{\pi z}{b}} - e^{-\frac{\pi(n+id)}{b}})(e^{\frac{\pi \bar{z}}{b}} - e^{-\frac{\pi(n-id)}{b}})(e^{\frac{\pi \bar{z}}{b}} - e^{\frac{\pi(n+id)}{b}})}{(e^{\frac{\pi z}{b}} - e^{\frac{\pi(n+id)}{b}})(e^{\frac{\pi z}{b}} - e^{-\frac{\pi(n-id)}{b}})(e^{\frac{\pi \bar{z}}{b}} - e^{-\frac{\pi(n+id)}{b}})(e^{\frac{\pi \bar{z}}{b}} - e^{\frac{\pi(n-id)}{b}})} \\ &+ \Im(z) \frac{\mathcal{V}}{b}. \quad (21) \end{aligned}$$

4 Infinite grids

We mentioned before that as $N \rightarrow \infty$ the series (or product) describing the potential does not seem to be explicitly summable. Suppose we wish to numerically find the potential of an “infinite” wire grid, characterized by the property of translational invariance: each of its

⁶We explicitly include λ as a variable here, so that all parameters are accounted for.

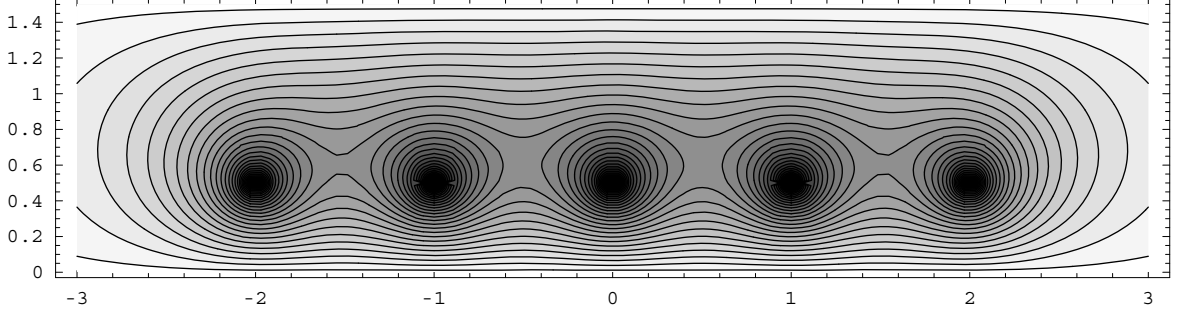


Figure 3: Contour plot of $V_g(x + iy; N = 2, b = 1.5, d = 0.5, \mathcal{V} = 0, \lambda = 1)$.

“cells” look identical. A reasonable procedure would be to pick some large N and look at the V_g in the center cell,⁷ $-0.5 \geq x \geq 0.5$. We know N is sufficiently large when,

1. the further contribution from the terms with $n > N$ is very small, or,
2. the center cell is virtually identical to those surrounding it.

4.1 Condition 1

Let’s begin with the first condition. We wish to know the behavior of,

$$T = \lambda \log \left[\frac{(e^{\frac{\pi z}{b}} - e^{\frac{\pi(n-id)}{b}})(e^{\frac{\pi z}{b}} - e^{-\frac{\pi(n+id)}{b}})(e^{\frac{\pi \bar{z}}{b}} - e^{-\frac{\pi(n-id)}{b}})(e^{\frac{\pi \bar{z}}{b}} - e^{\frac{\pi(n+id)}{b}})}{(e^{\frac{\pi z}{b}} - e^{\frac{\pi(n+id)}{b}})(e^{\frac{\pi z}{b}} - e^{-\frac{\pi(n-id)}{b}})(e^{\frac{\pi \bar{z}}{b}} - e^{-\frac{\pi(n+id)}{b}})(e^{\frac{\pi \bar{z}}{b}} - e^{\frac{\pi(n-id)}{b}})} \right] \quad (22)$$

for fixed x, y, b, d and large n (this is just series term in Eq. (20), with $z = x + iy$). Some numerical tests suggest that $T \sim e^{-\pi n/b}$. To prove this claim, we look at,

$$\lim_{n \rightarrow \infty} \frac{T}{e^{-\frac{\pi n}{b}}}. \quad (23)$$

In this limit, both the numerator and denominator go to 0, so we may use L’Hôpital’s rule and differentiate both. This gets rid of the logarithm in T and makes the limit slightly more

⁷In this entire section we ignore the \mathcal{V} term in V_g , *i.e.* we assume that both conducting planes are grounded. We are investigating the errors of various approximations to the infinite sum, and we concern ourselves only with the terms of this sum. The free \mathcal{V} term does not affect these calculations at all.

manageable to evaluate. After some algebra (done with *Mathematica*,⁸) we find that,

$$\begin{aligned}
\frac{\partial T}{\partial n} &= \lambda \frac{\pi}{b} \left[e^{\frac{(-id+n)\pi}{b}} (-1 + e^{\frac{2id\pi}{b}}) (-1 + e^{\frac{2n\pi}{b}}) (e^{\frac{\pi(x-iy)}{b}} - e^{\frac{\pi(x+iy)}{b}}) (-e^{\frac{2n\pi}{b}} + e^{\frac{2\pi x}{b}} + e^{\frac{4\pi x}{b}} + 3e^{\frac{2\pi(n+x)}{b}} \right. \\
&\quad + e^{\frac{4\pi(n+x)}{b}} + e^{\frac{2\pi(n-id+x)}{b}} + e^{\frac{2\pi(id+n+x)}{b}} + e^{\frac{2\pi(2n+x)}{b}} + 3e^{\frac{2\pi(n+2x)}{b}} + e^{\frac{2\pi(n-id+2x)}{b}} + e^{\frac{2\pi(n+id+2x)}{b}} \\
&\quad - e^{\frac{2\pi(n+3x)}{b}} + e^{\frac{2\pi(n+x-iy)}{b}} + e^{\frac{2\pi(n+2x-iy)}{b}} - 2e^{\frac{\pi(n-id+3x-iy)}{b}} - 2e^{\frac{\pi(n+id+3x-iy)}{b}} - 2e^{\frac{\pi(3n+id+3x-iy)}{b}} \\
&\quad + e^{\frac{2\pi(n+x+iy)}{b}} + e^{\frac{2\pi(n+2x+iy)}{b}} - 2e^{\frac{\pi(n-id+3x+iy)}{b}} - 2e^{\frac{\pi(n+id+3x+iy)}{b}} - 2e^{\frac{\pi(3n-id+3x+iy)}{b}} \\
&\quad \left. - 2e^{\frac{\pi(3n+id+3x+iy)}{b}} - 2e^{-\frac{i\pi(d+3in+3ix+y)}{b}} \right] \\
&\div \left[(e^{\frac{(n-id)\pi}{b}} - e^{\frac{\pi(x-iy)}{b}}) (-e^{\frac{(n+id)\pi}{b}} + e^{\frac{\pi(x-iy)}{b}}) (-1 + e^{\frac{\pi(n-id+x-iy)}{b}}) (-1 + e^{\frac{\pi(n+id+x-iy)}{b}}) \right. \\
&\quad \left. \times (e^{\frac{(n-id)\pi}{b}} - e^{\frac{\pi(x+iy)}{b}}) (e^{\frac{(n+id)\pi}{b}} - e^{\frac{\pi(x+iy)}{b}}) (-1 + e^{\frac{\pi(n-id+x+iy)}{b}}) (-1 + e^{\frac{\pi(n+id+x+iy)}{b}}) \right]. \quad (24)
\end{aligned}$$

For large n , we keep only the largest exponent in each factor, and anything it is multiplied by. The long sum in the denominator contains only two terms $\sim e^{\frac{4\pi n}{b}}$ (the fastest growing ones); the rest of the terms are removed. In the end, this results in $\partial T/\partial n \sim e^{-\frac{\pi n}{b}}$, which is cancelled by $\partial/\partial n(e^{-\frac{\pi n}{b}})$ from the denominator of Eq. (23). The terms that decrease more slowly would have gone to zero in Eq. (23) for large n , so their removal is justified. We have:

$$\begin{aligned}
\frac{\frac{\partial T}{\partial n}}{\frac{\partial}{\partial n}(e^{-\frac{\pi n}{b}})} &\approx \frac{\lambda \left(\frac{\pi}{b}\right) (e^{\frac{(-id+n)\pi}{b}}) (-1 + e^{\frac{2id\pi}{b}}) (e^{\frac{2n\pi}{b}}) (e^{\frac{\pi(x-iy)}{b}} - e^{\frac{\pi(x+iy)}{b}}) (e^{\frac{4\pi(n+x)}{b}} + e^{\frac{2\pi(2n+x)}{b}})}{(e^{\frac{(n-id)\pi}{b}}) (-e^{\frac{(n+id)\pi}{b}}) (e^{\frac{\pi(n-id+x-iy)}{b}}) (e^{\frac{\pi(n+id+x-iy)}{b}}) (e^{\frac{(n-id)\pi}{b}}) (e^{\frac{(n+id)\pi}{b}}) (e^{\frac{\pi(n-id+x+iy)}{b}}) (e^{\frac{\pi(n+id+x+iy)}{b}})} \\
&\quad \left(-\frac{\pi}{b}\right) e^{-\frac{\pi n}{b}} \\
&= \frac{-\lambda e^{\frac{7\pi n}{b}} (e^{\frac{\pi(-id+3x-iy)}{b}}) (e^{\frac{2\pi id}{b}} - 1) (e^{\frac{2\pi x}{b}} + 1) (e^{\frac{2\pi iy}{b}} - 1)}{e^{\frac{8\pi n}{b}} (e^{\frac{4\pi x}{b}})} \\
&= -\lambda e^{-\frac{\pi(x+iy+id)}{b}} (e^{\frac{2\pi id}{b}} - 1) (e^{\frac{2\pi x}{b}} + 1) (e^{\frac{2\pi iy}{b}} - 1) \\
&= 8\lambda \sin\left(\frac{\pi d}{b}\right) \cosh\left(\frac{\pi x}{b}\right) \sin\left(\frac{\pi y}{b}\right). \quad (25)
\end{aligned}$$

Therefore,

$$\lim_{n \rightarrow \infty} \frac{T}{e^{-\frac{\pi n}{b}}} = 8\lambda \sin\left(\frac{\pi d}{b}\right) \cosh\left(\frac{\pi x}{b}\right) \sin\left(\frac{\pi y}{b}\right), \quad (26)$$

and

$$T \approx 8\lambda \sin\left(\frac{\pi d}{b}\right) \cosh\left(\frac{\pi x}{b}\right) \sin\left(\frac{\pi y}{b}\right) e^{-\frac{\pi n}{b}} \quad (27)$$

for large n .

Using this approximation, we can now explicitly sum the tail end of the series in Eq. (20),

$$\begin{aligned}
\lambda \sum_{n=N+1}^{\infty} \log[\dots] &\approx 8\lambda \sin\left(\frac{\pi d}{b}\right) \cosh\left(\frac{\pi x}{b}\right) \sin\left(\frac{\pi y}{b}\right) \sum_{n=N+1}^{\infty} e^{-\frac{\pi n}{b}} \\
&= 8\lambda \sin\left(\frac{\pi d}{b}\right) \cosh\left(\frac{\pi x}{b}\right) \sin\left(\frac{\pi y}{b}\right) \frac{e^{-\frac{\pi N}{b}}}{e^{\frac{\pi}{b}} - 1}. \quad (28)
\end{aligned}$$

⁸Not much effort was put into simplifying the appearance of this formula, since we remove most of the terms in the next step.

Call this “error term” E . This is a good approximation of the tail end so long as $e^{-\frac{\pi N}{b}} (e^{\frac{\pi}{b}} - 1)^{-1}$ is small (ensuring our N is sufficiently large). In the center cell, the region $-\frac{1}{2} \leq x \leq \frac{1}{2}$, $0 \leq y \leq b$, we have,

$$|E| \leq 8|\lambda| \frac{e^{-\frac{\pi N}{b}}}{e^{\frac{\pi}{b}} - 1} \cosh \frac{\pi}{2b}. \quad (29)$$

Suppose we would like $|E| < e^{-C}$ for some positive C , proportional to the digits of precision in our numerical approximation to the infinite grid. Solving for N we find that we need,

$$\begin{aligned} e^{-\frac{\pi N}{b}} &< \frac{1}{8|\lambda|} e^{-C} \frac{e^{\frac{\pi}{b}} - 1}{\cosh \frac{\pi}{2b}} \\ \Rightarrow N &> \frac{(C + \log 8|\lambda|)b}{\pi} - \frac{b}{\pi} \log(e^{\frac{\pi}{b}} - 1) + \frac{b}{\pi} \log \left(\cosh \frac{\pi}{2b} \right) \end{aligned} \quad (30)$$

For $b < 1$ (b small), we see that $-\frac{b}{\pi} \log(e^{\frac{\pi}{b}} - 1) \approx -\frac{b}{\pi} \log(e^{\frac{\pi}{b}}) = -1$. Also,

$$\frac{b}{\pi} \log \left(\cosh \frac{\pi}{2b} \right) = \frac{b}{\pi} \log \left(\frac{e^{\frac{\pi}{2b}} + e^{-\frac{\pi}{2b}}}{2} \right) \approx \frac{b}{\pi} \log \left(\frac{e^{\frac{\pi}{2b}}}{2} \right) = \frac{1}{2} - \frac{b}{\pi} \log 2, \quad (31)$$

So we may write the condition on N as,

$$N \gtrsim \frac{(C + \log 4|\lambda|)b}{\pi} - \frac{1}{2}, \quad b < 1. \quad (32)$$

For the case $b > 1$, we first observe that,

$$\begin{aligned} \lim_{b \rightarrow \infty} b^2 \log \left(\cosh \frac{\pi}{2b} \right) &= \lim_{b \rightarrow \infty} \frac{\frac{d}{db} \log \left(\cosh \frac{\pi}{2b} \right)}{\frac{d}{db} b^2} \\ &= \lim_{b \rightarrow \infty} \frac{\pi}{4} b \tanh \frac{\pi}{2b} \\ &= \lim_{b \rightarrow \infty} \frac{\pi}{4} b \left[\frac{\pi}{2b} + O \left(\frac{1}{b^3} \right) \right] \\ &= \frac{\pi^2}{8}. \end{aligned} \quad (33)$$

So $\frac{b}{\pi} \log \left(\cosh \frac{\pi}{2b} \right) \sim \frac{\pi}{8b}$ for large b . Indeed, the approximation is already good for $b \approx 1$, and we always have $\frac{b}{\pi} \log \left(\cosh \frac{\pi}{2b} \right) < \frac{\pi}{8b}$. We can also approximate,

$$\begin{aligned} -\frac{b}{\pi} \log(e^{\frac{\pi}{b}} - 1) &= -\frac{b}{\pi} \log \left[\frac{\pi}{b} + O \left(\frac{1}{b^2} \right) \right] \\ &\approx \frac{b}{\pi} \log \left(\frac{b}{\pi} \right), \end{aligned} \quad (34)$$

and (with some algebra left out),

$$\begin{aligned}
\lim_{b \rightarrow \infty} -\frac{b}{\pi} \log(e^{\frac{\pi}{b}} - 1) - \frac{b}{\pi} \log\left(\frac{b}{\pi}\right) &= -\lim_{b \rightarrow \infty} \frac{b}{\pi} \log\left[\frac{b}{\pi} \left(e^{\frac{\pi}{b}} - 1\right)\right] \\
&= -\lim_{b \rightarrow \infty} \frac{\frac{d}{db} \log\left[\frac{b}{\pi} \left(e^{\frac{\pi}{b}} - 1\right)\right]}{\frac{d}{db} \frac{\pi}{b}} \\
&= \lim_{b \rightarrow \infty} \frac{b(e^{\frac{\pi}{b}} - 1) - \pi e^{\frac{\pi}{b}}}{\pi(e^{\frac{\pi}{b}} - 1)} \\
&= \lim_{b \rightarrow \infty} \frac{b \left[\frac{\pi}{b} + \frac{\pi^2}{2b} + O\left(\frac{1}{b^3}\right)\right] - \pi \left[1 + \frac{\pi}{b} + O\left(\frac{1}{b^2}\right)\right]}{\pi \left[\frac{\pi}{b} + O\left(\frac{1}{b^2}\right)\right]} \\
&= \lim_{b \rightarrow \infty} \frac{-\frac{\pi^2}{2} + O\left(\frac{1}{b}\right)}{\pi^2 + O\left(\frac{1}{b}\right)} \\
&= -\frac{1}{2}. \tag{35}
\end{aligned}$$

Over the entire range $b > 1$,

$$-\frac{b}{\pi} \log(e^{\frac{\pi}{b}} - 1) \approx \frac{b}{\pi} \log\left(\frac{b}{\pi}\right) - \frac{1}{2} \tag{36}$$

is a *very* good approximation. Our condition for large N may be written as,

$$N \gtrsim \frac{(C + \log 8|\lambda|)b}{\pi} + \frac{b}{\pi} \log\left(\frac{b}{\pi}\right) + \frac{\pi}{8b} - \frac{1}{2}, \quad b > 1 \tag{37}$$

(And of course, for very large b , we may drop the $\frac{\pi}{8b}$ term.)

Figure 4 shows the two approximations to Eq. (30), for parameters $C = 3$ and $|\lambda| = 1$.

4.2 Condition 2

We have not said much about the second condition for N to be sufficiently large, namely that the center cell is virtually identical to those surrounding it. Such a test can easily be done visually by looking at a contour plot of V_g . It is rather apparent when contours close to the edge are not periodic in x .

Analytically, we would like $V_g(x+iy) = V_g(x+1+iy)$ ⁹ for x in the the center cell (note $x \pm 1$ are equivalent, since V_g is symmetric). If we consider the difference $V_g(x+iy) - V_g(x+1+iy)$, and separate the potential contributions coming from symmetrically opposed ($\pm n$) wires, we see that most of the terms of Eq. (20) vanish. We are left with,

$$V_g(x+iy) - V_g(x+1+iy) = [\text{potential from } +N] - [\text{potential from } -(N+1)]. \tag{38}$$

⁹The other parameters have been suppressed for simplicity.

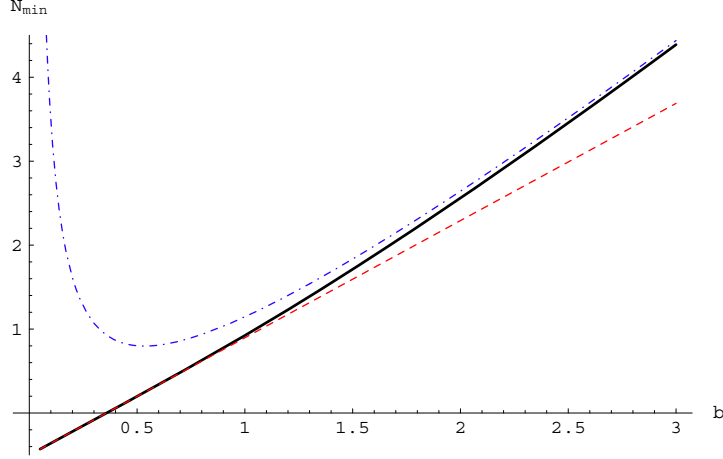


Figure 4: The “cutoff” for sufficiently large N . Approximation Eq. (32) is in dashed red, and Eq. (37) in dot-dashed blue.

Requiring that this difference be small is much the same as requiring that the contributions from large N terms be small, as we analyzed above for condition 1. Here, however, the actual difference may be much smaller than the individual terms themselves, a situation we will investigate.

From Eq. (27) we may infer that wires at positions $\pm n$ contribute a potential,

$$\begin{aligned} V_{\pm n}(x + iy) &\approx 4\lambda \sin\left(\frac{\pi d}{b}\right) \left(e^{\pm \frac{\pi x}{b}}\right) \sin\left(\frac{\pi y}{b}\right) e^{-\frac{\pi n}{b}} \\ &= 4\lambda \sin\left(\frac{\pi d}{b}\right) \sin\left(\frac{\pi y}{b}\right) e^{-\frac{\pi(n \mp x)}{b}} \end{aligned} \quad (39)$$

to the region near the center. We would like, then, that,

$$\begin{aligned} V_N(x + iy) - V_{-(N+1)}(x + iy) &\approx 4\lambda \sin\left(\frac{\pi d}{b}\right) \sin\left(\frac{\pi y}{b}\right) \left[e^{-\frac{\pi(N-x)}{b}} - e^{-\frac{\pi((N+1)+x)}{b}}\right] \\ &= 8\lambda \sin\left(\frac{\pi d}{b}\right) \sin\left(\frac{\pi y}{b}\right) \sinh\left(\frac{\pi(x + 1/2)}{b}\right) e^{-\frac{\pi(N+1/2)}{b}} \end{aligned} \quad (40)$$

be small. In the center cell we have $-\frac{1}{2} \leq x \leq \frac{1}{2}$, so the sinh term is at most $\sinh\left(\frac{\pi}{b}\right)$. Calling the difference D , we obtain,

$$|D| \leq 8|\lambda| \sinh\left(\frac{\pi}{b}\right) e^{-\frac{\pi(N+1/2)}{b}}, \quad (41)$$

and if we want this to be less than some parameter e^{-K} (where K proportional to the digits of correlation between two adjacent cells) we need,

$$N \gtrsim \frac{(K + \log 8|\lambda|)b}{\pi} + \frac{b}{\pi} \log\left(\sinh\left(\frac{\pi}{b}\right)\right) - \frac{1}{2}. \quad (42)$$

This time, having a large b seems to be in our favor! The function in Eq. (42) starts at $+1/2$ (for $b = 0$), increases to a maximum, and then decreases as b gets large. However, we find numerically¹⁰ that the location of this maximum goes as $\pi e^{K+\log(8|\lambda|)-1} = 8\pi|\lambda|e^{K-1}$, and that the height of the maximum goes as $8|\lambda|e^{K-1} - \frac{1}{2}$. Thus, in general, it would take an extremely large b to benefit from this effect – much too large for Eq. (37), and (intuitively) too large for the physical situation.¹¹

We may consider two approximations to Eq. (42). For small b we have $\sinh \frac{\pi}{b} \approx \frac{1}{2}e^{\frac{\pi}{b}}$, so we obtain,

$$N \gtrsim \frac{(K + \log 4|\lambda|)b}{\pi} + \frac{1}{2}, \quad (43)$$

which seems to be very good for $b \leq 1$ and reasonably good up to $b \leq 2$. For large b , $\sinh \frac{\pi}{b} \approx \frac{\pi}{b}$, so $\frac{b}{\pi} \log \left(\sinh \frac{\pi}{b} \right) \approx -\frac{b}{\pi} \log \frac{b}{\pi}$. Correcting this (somewhat arbitrarily)¹² by $\frac{\pi}{8b}$ we arrive at,

$$N \gtrsim \frac{(K + \log 8|\lambda|)b}{\pi} - \frac{b}{\pi} \log \left(\frac{b}{\pi} \right) + \frac{\pi}{8b} - \frac{1}{2}. \quad (44)$$

Figure 5 shows a graph of Eq. (42), with its two approximations, for $K = 3$ and $|\lambda| = 1$.

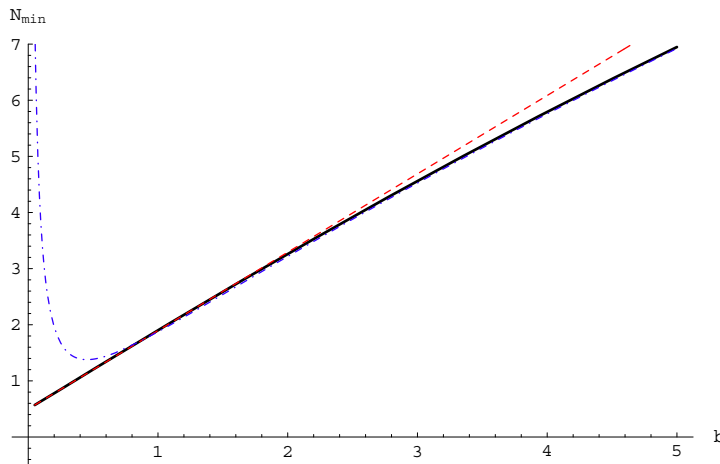


Figure 5: “Cutoff” for sufficiently large N , using the second condition. Eq. (43) is in dashed red, and Eq. (44) in dot-dashed blue.

4.3 Evaluation

In practice, it seems easy enough to just use Eq. (30) or Eq. (42) to determine a sufficiently large value of N . The approximations, however, were done to elucidate the general dependence of “large N ” on the various parameters. Both Eq. (32) and Eq. (43) show a linear

¹⁰Or, for large b , we could also use $\frac{b}{\pi} \log \left(\sinh \frac{\pi}{b} \right) \approx -\frac{b}{\pi} \log \left(\frac{b}{\pi} \right)$

¹¹See also the following section.

¹²In fact, $\lim_{b \rightarrow \infty} b \left(\frac{b}{\pi} \log \left(\sinh \frac{\pi}{b} \right) + \frac{b}{\pi} \log \frac{b}{\pi} \right) = \frac{\pi}{6}$. But we are more concerned with behavior for moderately-sized b , not the limit. So we use $\frac{\pi}{8b}$ instead of $\frac{\pi}{6b}$ because it fits this range better.

dependence for small b . It is indeed comforting to see how nearly identical these equations are for $C = K$, having the same multiplicative factor,

$$\frac{C + \log 8|\lambda|}{\pi} \tag{45}$$

and differing only by a constant 1. We can also see much similarity in Eq. (37) and Eq. (44); they differ by a sign. For moderately sized b , K (or C), and $|\lambda|$, they are basically equivalent, depending linearly on b with the same factor as Eq. (32) and Eq. (43).¹³

For much larger b , Eq. (44) (or Eq. (42)) seems somewhat unrealistic: N should always *increase* with increasing b . Indeed, for very large b we are no longer dealing with a wire between two plates. The plates are so far apart that we really only have an isolated grid. And for such large b , with $N \lesssim b$ as Eq. (42) would allow, the approximations that we made to derive Eq. (27) should no longer hold! The most dependable condition on N for very large b thus seems to be Eq. (37) with a positive $b \log b$ term.

We might also note that all equations show the same dependence on $|\lambda|$, which is hardly surprising. It might however be slightly confusing that for sufficiently small $|\lambda|$ the multiplicative coefficient Eq. (45) becomes negative. But, one must remember that C and K are absolute measures of precision (or error); indeed, the absolute error is comparable to e^{-C} (or e^{-K}). We may rewrite Eq. (45) as,

$$\frac{1}{\pi} \log \left(\frac{8|\lambda|}{e^{-C}} \right). \tag{46}$$

For a smaller $|\lambda|$ we want better precision. Putting the absolute error proportional to $|\lambda|$, the argument of the logarithm becomes a constant, typically much greater than 1.

4.4 Remarks

Before moving on, it might be beneficial (or interesting) to say a few more things about the formulas we have derived, in particular Eqs. 27 and 39. The latter implies that *at large distances* the potential of a wire sandwiched between two grounded conducting planes is,

$$V_w(\xi, y; b, d, \lambda) \approx 4\lambda \sin \left(\frac{\pi d}{b} \right) \sin \left(\frac{\pi y}{b} \right) e^{-\frac{\pi|\xi|}{b}}, \tag{47}$$

where ξ is the horizontal distance from the wire. (The wire is at height d between two planes a distance b apart, as usual).¹⁴ First, we notice that this potential is completely symmetric about $y = b/2$. It is zero on the conducting planes and “bulges out” symmetrically in the space between them. This is what we might have expected at large distances.

But we also notice that the ξ dependence is exponentially decreasing – somewhat remarkable in light of the fact that the potential of a wire in free space would grow logarithmically

¹³That’s the main point to get here, and it might be emphasized again: most of the time the dependence on b is essentially linear, with multiplicative factor Eq. (45).

¹⁴We might have derived Eq. (47) directly from Eq. (18), and then used it to write Eq. (39) and to derive Eq. (27). This would probably have been somewhat easier and more straightforward than the derivation in Section 4.1.

forever. This of course is entirely the effect of the grounded conducting planes: they *force* the potential to 0, and evidently they do so exponentially. (Note the b dependence in the exponential term.)

One other interesting result is that Eq. (18) essentially gives the potential of an infinite (vertical!) grid of wires in free space with *alternating* charges. The image wire we used to find the potential in the unit circle becomes an infinite grid of image wires in our regular space. From Eq. (18), let,

$$V_w(z; b, d, \lambda) = \lambda \log \left[\frac{(e^{\frac{\pi z}{b}} - e^{-\frac{i\pi d}{b}})(e^{\frac{\pi \bar{z}}{b}} - e^{\frac{i\pi d}{b}})}{(e^{\frac{\pi z}{b}} - e^{\frac{i\pi d}{b}})(e^{\frac{\pi \bar{z}}{b}} - e^{-\frac{i\pi d}{b}})} \right]. \quad (48)$$

If for some point $z = x + iy$ we let $y \mapsto 2b - y$ we effectively get $z \mapsto \bar{z}$; the numerator and denominator in Eq. (48) are switched, giving the logarithm and the overall potential a minus sign. If instead we let $y \mapsto y + 2b$, we effectively get $z \mapsto z$; the potential doesn't change.

Putting $d = b/2$ we obtain an infinite vertical grid with alternating charges and all wires the same distance (b) apart. (Otherwise, our “images” also alternate in their placement, as shown by the transformations above.) Figure 6 shows a contour plot of $V_w(x + iy; b, d, \lambda) = V_g(x, y; N = 0, b, d, \mathcal{V} = 0, \lambda)$, extended along the y direction so we may see the “image” grid.

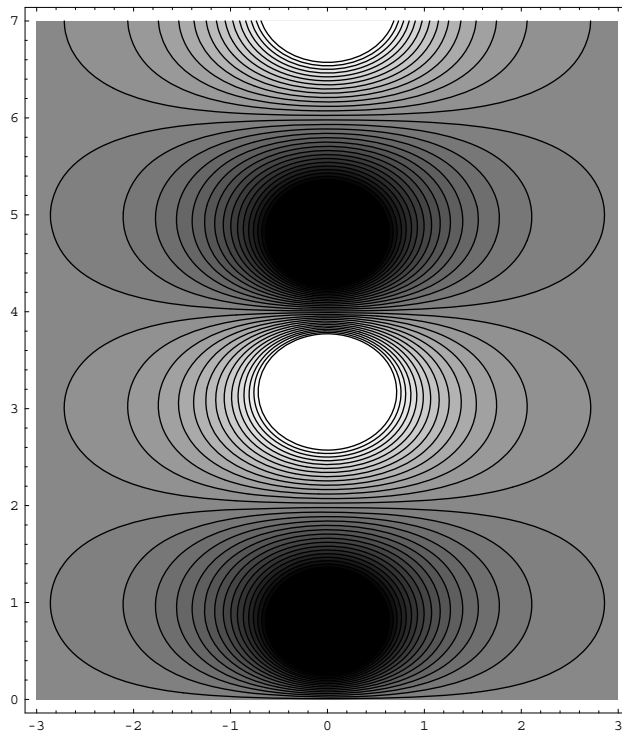


Figure 6: The vertical image grid; here, $\lambda = 1$, $b = 2$, and $d = 0.7$.

5 Multiple realistic grids and boundary conditions: an attempt at modelling

For practical modelling applications¹⁵, we are often interested in several wire grids placed between “infinite” conducting plates. Equation (12) gives a general expression for this (once we add in a potential $\frac{\mathcal{V}}{b}\Im(z)$); but we want to satisfy some specific boundary conditions, effectively to determine the correct combination of coefficients λ_k . We shall assume here that all grids involved in our problem have the same pitch, thereby allowing us to use the rescaled potentials V_g shown in Eq. (21) and Eq. (20).¹⁶

In a real application we may want to specify either the potential of a wire grid or the electric field at points on the wires – wires of finite radius. How do we accommodate this? Our wires are infinitesimally small, and we specify the charge λ on them. But, in a very small neighborhood of a wire, the equipotentials are almost perfect circles, as can be seen in Figs. 3 and 6. Thus we might approximate real wires of very small radius r with infinitesimal wires carrying an appropriate charge. (We evaluate the accuracy of this approximation further below.)

Then, another concern arises: if we approximate a small- N finite grid of real wires with a grid of infinitesimally small wires, the “circular” equipotentials at a small distance r from our infinitesimal wires won’t all have the same value! The wires at the ends of the grid will probably have a smaller potential than the wires in the middle. We could adjust Eq. (20) so that each term in the sum carried a *different* coefficient λ , as appropriate to keep the r -potentials constant. This may indeed be the necessary path to take in some situations! However, in many real cases N is very large, and, more importantly, N/b might be large. We can approximate the real grids by infinite grids, and in turn approximate the infinite “real” grids by our modelled finite grids with large N . For an infinite grid, the r -potentials will of course be constant. We therefore take N sufficiently large, as called for by the analysis of Section 4, and only consider the central cell of our grids.¹⁷

Now suppose we would like:

1. K grids¹⁸ placed at vertical positions d_1, \dots, d_K between two plates of separation b ,
2. wire radii r_k on the k th grid,
3. a potential difference \mathcal{V} between the top and bottom plates, and either
 - 4a. a potential v_k on each wire of the k th grid, or,
 - 4b. an electric field E_k at (say) the bottommost part of each wire of the k th grid.

¹⁵*Eg.* particle detectors

¹⁶In some problems, this is not the case; the argument given here may be adjusted accordingly.

¹⁷We are making *many* approximations. Perhaps better approximations exist, but in this way *are* getting a relatively simple, somewhat accurate model and some decent estimates. As noted further below, actual experiment will show whether or not we have done right.

¹⁸We are assuming here that the pitch of each grid is 1; otherwise the entire set specifications may be scaled appropriately.

We are assuming here that the pitch of each grid is 1; otherwise the entire set specifications may be scaled appropriately. Also we assume for the remainder of the section that $V_g[z; n, b, d]$ implicitly means $V_g[z; n, b, d, \mathcal{V} = 0, \lambda = 1]$, as given by Eq. (20). We shall put in \mathcal{V} and constants λ explicitly.

Specifying the electric field at the bottommost point of a wire requires that we know something of the “vertical” derivative of V_g . This calculation is carried out at the end of this section. For now, we simply refer to,

$$D_y V_g(z; n, b, d) := \frac{\partial}{\partial y} V_g(x + iy; n, b, d). \quad (49)$$

We fix some N , presumably satisfying,

$$N \gtrsim \frac{(C + \log 4\lambda)b}{\pi} \quad (50)$$

(or the appropriate large b equation) for some moderately sized C . We will not actually *specify* N here, and its actual value may be adjusted at the end.

5.1 $K = 1$, one grid

Suppose we only have one grid between the plates (so we may drop subscripts from the parameters). The general form of our potential is,

$$V(x, y) = \lambda V_g(x + iy; N, b, d) + \mathcal{V} \frac{y}{b}, \quad (51)$$

with λ a parameter to be determined. If the grid is at potential v , we would like,

$$V(\pm r, d) = \lambda V_g(\pm r + id; N, b, d) + \mathcal{V} \frac{d}{b} = v. \quad (52)$$

In other words, we are requiring that the potential at the (supposedly small) wire radius r be v . Since the potential may actually vary a little bit as we go around the wire, we just (somewhat arbitrarily) use the positions to the sides of the central wire as our boundary condition points. (It doesn't matter whether we use $+r$ or $-r$; recall that the potential is symmetric in x .) This determines.

$$\lambda^{(v)} = \frac{v - \mathcal{V}d/b}{V_g(\pm r + id; N, b, d)}. \quad (53)$$

If instead of condition 4a we use 4b, specifying the field at (again somewhat arbitrarily) the bottommost point of the central wire, we must have,

$$-D_y V(0, d - r) = -\lambda D_y V_g(i(d - r); N, b, d) - \frac{\mathcal{V}}{b} = E, \quad (54)$$

which fixes λ as,

$$\lambda^{(E)} = -\frac{E + \mathcal{V}/b}{D_y V_g(i(d - r); N, b, d)}. \quad (55)$$

5.2 $K > 1$, multiple grids

With multiple grids the general expression of the potential takes the form,

$$V(x, y) = \sum_{k=1}^K \lambda_k V_g(x + iy; N, b, d_k) + \mathcal{V} \frac{y}{b}, \quad (56)$$

and when imposing the potential or field conditions at the wires we obtain a system of K equations which look either like,

$$V(\pm r_j, d_j) = \sum_{k=1}^K \lambda_k V_g(\pm r_j + id_j; N, b, d_k) + \mathcal{V} \frac{d_j}{b} = v_j \quad (57)$$

(for potentials v_j on the j th grids) or,

$$-D_y V(0, d_j - r_j) = \sum_{k=1}^K \lambda_k [-D_y V_g(i(d_j - r_j); N, b, d_k)] - \frac{\mathcal{V}}{d} = E_j \quad (58)$$

(for fields E_j on the j th grids), with $j = 1, \dots, K$.

This system of equations is linear, and may be recast as,

$$\mathbf{M} \lambda = \mathbf{F} \quad (59)$$

$$\text{or } \sum_k M_{jk} \lambda_k = F_j, \quad (60)$$

where,

$$\lambda = (\lambda_1, \lambda_2, \dots, \lambda_K)^t, \quad (61)$$

$$F_j = \begin{cases} v_j - \mathcal{V} \frac{d_j}{b} & \text{if potential condition on } j\text{th grid} \\ E_j + \frac{\mathcal{V}}{b} & \text{if field condition on } j\text{th grid,} \end{cases} \quad (62)$$

$$M_{jk} = \begin{cases} V_g(\pm r_j + id_j; N, b, d_k) & \text{if potential condition on } j\text{th grid} \\ -D_y V_g(i(d_j - r_j); N, b, d_k) & \text{if field condition on } j\text{th grid.} \end{cases} \quad (63)$$

The coefficients λ_k may then be solved for by the usual method of determinants. This, then, is a complete solution to the problem we posed.

5.3 An example

In a certain particle detector we have the following configuration:

- A fine mesh (approximated by a plane) at position 0 mm and (negative) potential \mathcal{V} ,
- A grid (1), pitch 2 mm, radius 0.0100 mm, at position 9.80 mm and potential \mathcal{V}_1 ,
- A grid (2), pitch 2 mm, radius 0.0625 mm, at position 12.62 mm and potential 0,

- A fine mesh (approximated by a plane) at position 19.48 mm and potential 0.¹⁹

To fit the analysis we have been performing, we may add a potential $-\mathcal{V}$ to everything and divide all quantities by 2 so that the pitch is 1 mm. This results in:

- A fine mesh (approximated by a plane) at position 0 mm and potential 0,
- A grid (1), pitch 1 mm, radius 0.0050 mm, at position 4.90 mm and potential v_1 ,
- A grid (2), pitch 1 mm, radius 0.0312 mm, at position 6.31 mm and potential v_2 ,
- A fine mesh (approximated by a plane) at position 9.74 mm and potential v_2 ,

with $v_1 = (\mathcal{V}_1 - \mathcal{V})/2$ and $v_2 = -\mathcal{V}/2$.

Our problem is one of transparency. While keeping \mathcal{V} (v_2) fixed, we wish to vary the value of \mathcal{V}_1 (v_1) so that the detector is either fully transparent to drifting electrons or fully intercepting of them at grid 1. We assume the detector is fully transparent when $E_1 = 0$, *i.e.* the field at the bottommost point of grid 1 is 0. And the detector is fully intercepting when $v_1 = v_2$.²⁰

We may begin with full transparency. In this case we have,

$$\mathbf{M} = \begin{pmatrix} -D_y V_g((4.9 - 0.005)i; N, 9.74, 4.9) & -D_y V_g((4.9 - 0.005)i; N, 9.74, 6.31) \\ V_g(\pm 0.0312 + 6.31 i; N, 9.74, 4.9) & V_g(\pm 0.0312 + 6.31 i; N, 9.74, 6.31) \end{pmatrix}, \quad (64)$$

$$\mathbf{F} = \begin{pmatrix} v_2/9.74 \\ v_2(1 - 6.31/9.74) \end{pmatrix}, \quad (65)$$

and,

$$\lambda_1 = \frac{\det \begin{pmatrix} v_2/9.74 & -D_y V_g((4.9 - 0.005)i; N, 9.74, 6.31) \\ v_2(1 - 6.31/9.74) & V_g(\pm 0.0312 + 6.31 i; N, 9.74, 6.31) \end{pmatrix}}{\det(\mathbf{M})},$$

$$\lambda_2 = \frac{\det \begin{pmatrix} -D_y V_g((4.9 - 0.005)i; N, 9.74, 4.9) & v_2/9.74 \\ V_g(\pm 0.0312 + 6.31 i; N, 9.74, 4.9) & v_2(1 - 6.31/9.74) \end{pmatrix}}{\det(\mathbf{M})}. \quad (66)$$

If we would like a precision in our infinite grid estimate proportional to (say) ~ 4 digits when $\max(\lambda_1, \lambda_2) = 1$, we should take,

$$N \gtrsim \left(\log \frac{8}{e^{-4}} \right) \frac{9.74}{\pi} = 18.85 \quad (67)$$

¹⁹The idea here is that most drifting electrons will be collected on grid 2, but any that get through will be collected on the 0V mesh.

²⁰These conditions, in a sense, give estimates of the *minimum* voltages we will have to apply to grid 1 to result in either transparency or interception.

Putting $N = 20$, then, we obtain,

$$\lambda_1 = -3.847 \times 10^{-4} v_2, \quad \lambda_2 = 1.157 \times 10^{-2} v_2. \quad (68)$$

Therefore our potential is,

$$\begin{aligned} V(x, y) = & -3.847 \times 10^{-4} v_2 V_g(x + iy; 20, 9.74, 4.9) \\ & + 1.157 \times 10^{-2} v_2 V_g(x + iy; 20, 9.74, 6.31) + (v_2/9.74)y. \end{aligned} \quad (69)$$

Figure 7 shows a plot of $V(0, y)$, the profile of the potential going through the central wire. One may imagine electrons climbing up the potential slope, which is essentially linear up to the second grid. The first grid is invisible on a large scale (as we might indeed want), and so is shown close up in the left plot. Note how the potential is flat at $y = 8.895$, as required. Figures 10-12 of the Appendix show contour plots of various sections of the grid. It was necessary to zoom in on the different sections in order to see the detail.

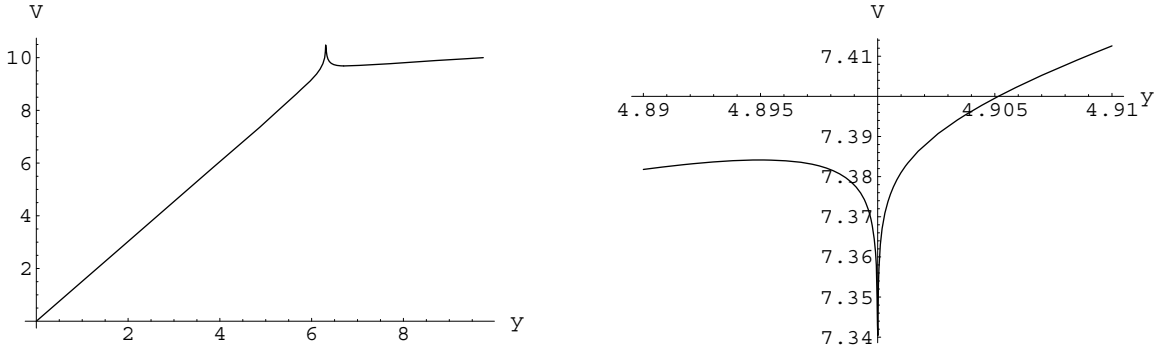


Figure 7: $V(0, y)$ transparent, with $v_2 = 10$.

Letting $x + iy = 4.9 \pm 0.005i$ (the outside of the central wire of grid 1), we get,

$$v_1 = V(4.9, 0.005) \approx 0.739 v_2. \quad (70)$$

Using our original notation, we see that,

$$\begin{aligned} \mathcal{V}_1 &= 2(v_1 - v_2) \\ \mathcal{V} &= -2v_2, \end{aligned} \quad (71)$$

and so,

$$\mathcal{V}_1 = \left(1 - \frac{v_1}{v_2}\right) \mathcal{V} \quad (72)$$

$$\approx 0.261 \mathcal{V} \quad (73)$$

in our case, for full transparency.

We would also like to find the potentials for the case of full interception (or full collection on grid 1). In this case, we require $v_1 = v_2$, or $\mathcal{V}_1 = 0$. We have,

$$\mathbf{M} = \begin{pmatrix} V_g(\pm 0.005 + 4.9i; N, 9.74, 4.9) & V_g(\pm 0.005 + 4.9i; N, 9.74, 6.31) \\ V_g(\pm 0.0312 + 6.31i; N, 9.74, 4.9) & V_g(\pm 0.0312 + 6.31i; N, 9.74, 6.31) \end{pmatrix}, \quad (74)$$

$$\mathbf{F} = \begin{pmatrix} v_2(1 - 4.9/9.74) \\ v_2(1 - 6.31/9.74) \end{pmatrix}. \quad (75)$$

Choosing $N = 20$ as above, these give (evaluating the determinants),

$$\begin{aligned} \lambda_1 &= 0.01124 \\ \lambda_2 &= 0.00349. \end{aligned} \quad (76)$$

Therefore, for full interception at grid 1, we have,

$$\begin{aligned} V(x, y) &= 0.01124 v_2 V_g(x + iy; 20, 9.74, 4.9) \\ &\quad + 0.00349 v_2 V_g(x + iy; 20, 9.74, 6.31) + (v_2/9.74)y. \end{aligned} \quad (77)$$

A plot of $V(0, y)$ is shown in Fig. 8, and a contour plot in Fig. 13. There is no need here to zoom in on details, since all the charges are moderately strong.

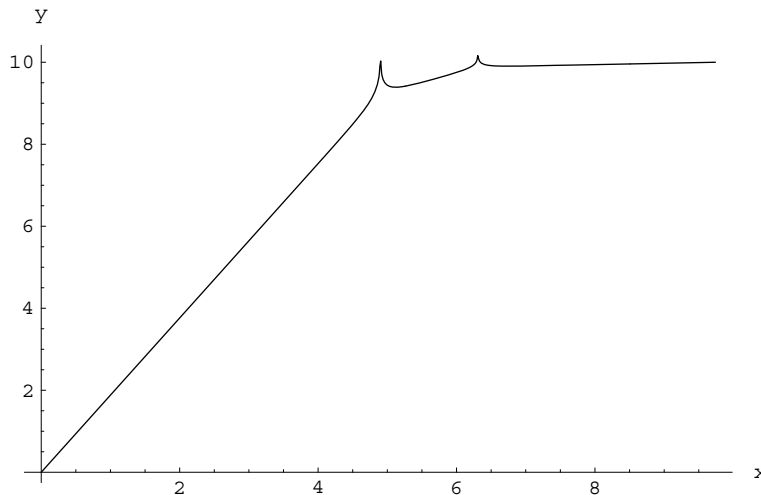


Figure 8: $V(0, y)$ intercepting, with $v_2 = 10$.

5.4 Some brief comments on error

As discussed at the beginning of this section, the approximations we have made in our model carry with them two major sources of error. The first comes from our infinite grid approximation. By choosing $N = 20$ we assured ourselves that, were we to have only one grid by itself, the potential of the center cell would be ‘correct’ to a few decimal places better

than λ of that grid. With *two* grids (or K grids), this error bound remains true for each grid individually. When they are superimposed we only know that the complete potential is accurate to a few decimal places less than the *largest* λ_k .²¹ In our two cases above, though, the values we obtained for λ_1 and λ_2 were roughly comparable (differing only by two or so orders of magnitude), and $N = 20$ gives an approximation to an infinite grid that is not bad at all. Figure 9 estimates the absolute error along the line $x = 0$ by comparing our potentials to those with $N = 50$.²²

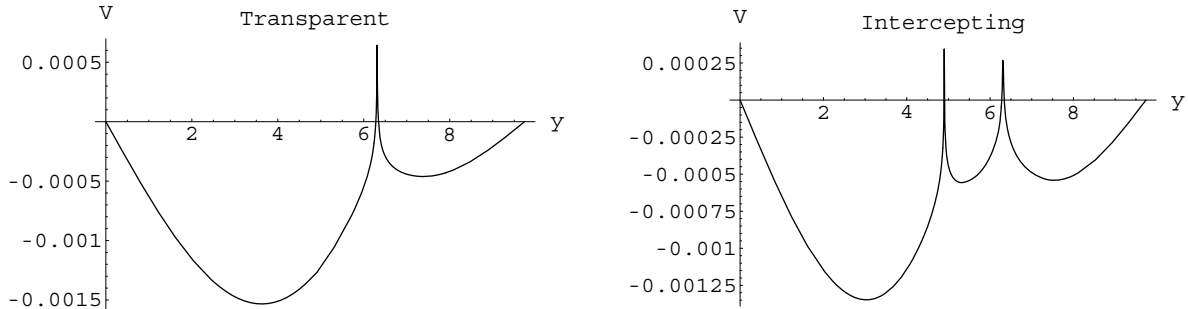


Figure 9: Estimate of absolute error in $V(0, y)$ (with $v_2 = 10$) vs. an infinite grid.

Unfortunately, there is a quite unknown error in our approximation of the real particle detector as a set of infinite grids (which we then approximated with our model). There is also error coming from the fact that we assumed our wire radii were small enough that we could approximate the wires by infinitesimally small ones. This is valid as long as computed equipotentials at the real wire radii are circular. In the case of an intercepting grid 1, this does seem to be the case, as one may see from Figure 13. But, in the case of transparency, this is *not* valid at grid 1, as can be seen in Figs. 7 and 11. In this case, the linear potential difference between the plates and the contribution from grid 2 effectively set up a (strong) linear potential (uniform field) at grid 1. When we add in the potential of grid 1, with very small λ_1 , this linear potential overpowers the tendency of equipotentials to be circular. The value of v_1 given in Eq. (70) is essentially just the value of the linear potential. To achieve full transparency in our real drift chamber, we will probably need a lower v_1 (or \mathcal{V}_1) than that calculated.

Some of the errors discussed here are small, while others may be quite significant. The model we have used might be adjusted slightly in different ways to try to improve its accuracy. But, in the end it will still only give a suggestion of what certain parameters need to be, as it

²¹It occurs to the author that *fractional* error may have been a good concept to explore. Perhaps another day.

²²The potentials for $N = 50$ use slightly corrected values of λ_1 and λ_2 , calculated with V_g and $D_y V_g$ with $N = 50$. It turns out that our $N = 20$ values were good to three significant digits, and ± 1 for the fourth significant digit. This slight alteration is what causes the sharp (infinite) peaks in the error graphs at the grids. We have been slightly naive, ignoring this correction, and predicting an absolute bound on error. But, the sharp peaks only manifest themselves near the *infinitesimally* small wires, well away from the finite wire bounds we are trying to model...

does now. Its ultimate validity must be tested experimentally. One must *try* the suggested value of \mathcal{V}_1 for transparency and *see* if transparency is indeed achieved! As mentioned, a lower value might be needed. (We may also need to use a higher value of \mathcal{V}_1 than 0, as called for by our heuristic, to achieve full interception.)²³

Hopefully our model will provide some helpful suggestions, both through its predictions of parameters and its ability to provide visualizations. However, whether or not this happens, we may content ourselves with the fact that it has provided an excellent exercise.

5.5 The y -derivative

For closure before we finish, we will explicitly compute $\frac{\partial}{\partial y} V_g(x + iy; n, b, d)$. From Eq. (20) we have,

$$V_g(x + iy; N, b, d) = \log \left[\frac{(e^{\frac{\pi(x-iy)}{b}} - e^{-\frac{i\pi d}{b}})(e^{\frac{\pi(x-iy)}{b}} - e^{\frac{i\pi d}{b}})}{(e^{\frac{\pi(x-iy)}{b}} - e^{\frac{i\pi d}{b}})(e^{\frac{\pi(x-iy)}{b}} - e^{-\frac{i\pi d}{b}})} \right] \quad (78)$$

$$+ \sum_{n=1}^N \log \left[\frac{(e^{\frac{\pi(x-iy)}{b}} - e^{\frac{\pi(n-id)}{b}})(e^{\frac{\pi(x-iy)}{b}} - e^{-\frac{\pi(n+id)}{b}})(e^{\frac{\pi(x-iy)}{b}} - e^{-\frac{\pi(n-id)}{b}})(e^{\frac{\pi(x-iy)}{b}} - e^{\frac{\pi(n+id)}{b}})}{(e^{\frac{\pi(x-iy)}{b}} - e^{\frac{\pi(n+id)}{b}})(e^{\frac{\pi(x-iy)}{b}} - e^{-\frac{\pi(n-id)}{b}})(e^{\frac{\pi(x-iy)}{b}} - e^{-\frac{\pi(n+id)}{b}})(e^{\frac{\pi(x-iy)}{b}} - e^{\frac{\pi(n-id)}{b}})} \right].$$

But letting,

$$V_w(x + iy; N, b, d) = \log \left[\frac{(e^{\frac{\pi(x-iy)}{b}} - e^{-\frac{i\pi d}{b}})(e^{\frac{\pi(x-iy)}{b}} - e^{\frac{i\pi d}{b}})}{(e^{\frac{\pi(x-iy)}{b}} - e^{\frac{i\pi d}{b}})(e^{\frac{\pi(x-iy)}{b}} - e^{-\frac{i\pi d}{b}})} \right] \quad (79)$$

(*c.f.*, Eq. (78)), we see from Eq. (14) (and common sense applied to our initial derivation) that we may write Eq. (78) as

$$\begin{aligned} V_g(x + iy; N, b, d) &= V_w(x + iy; N, b, d) + \sum_{n=1}^N [\text{potential from wires displaced } \pm n \text{ units}] \\ &= V_w(x + iy; N, b, d) \\ &\quad + \sum_{n=1}^N [V_w((x + n) + iy; N, b, d) + V_w((x - n) + iy; N, b, d)]. \end{aligned} \quad (80)$$

Then our derivative is,

$$\begin{aligned} \frac{\partial}{\partial y} V_g(x + iy; N, b, d) &= \frac{\partial}{\partial y} V_w(x + iy; N, b, d) \\ &\quad + \sum_{n=1}^N \left[\frac{\partial}{\partial y} V_w((x + n) + iy; N, b, d) + \frac{\partial}{\partial y} V_w((x - n) + iy; N, b, d) \right], \end{aligned} \quad (81)$$

and we see that the only function we really have to differentiate is V_w . After finding this derivative, we have simply to substitute $x \rightarrow x \pm n$ to obtain the terms in the sum. Using

²³Using contour plots such as Fig. 13, and creating plots of field lines, the model may in fact help us study the validity of the heuristic. . .

Mathematica and some further rearranging, we find,

$$\begin{aligned}
& \frac{\partial}{\partial y} V_w(x + iy; N, b, d) \\
&= \frac{i\pi}{b} \frac{e^{\frac{\pi(x-iy)}{b}} \left(e^{\frac{id\pi}{b}} - e^{\frac{-id\pi}{b}} \right) \left(1 + e^{\frac{2\pi x}{b}} + e^{\frac{\pi(2x+2iy)}{b}} + e^{\frac{2i\pi y}{b}} - 2e^{\frac{\pi(x+iy)}{b}} \left(e^{\frac{-id\pi}{b}} + e^{\frac{id\pi}{b}} \right) \right)}{\left(e^{\frac{\pi(x+iy)}{b}} - e^{\frac{id\pi}{b}} \right) \left(e^{\frac{\pi(x+iy)}{b}} - e^{\frac{-id\pi}{b}} \right) \left(e^{\frac{\pi(x-iy)}{b}} - e^{\frac{id\pi}{b}} \right) \left(e^{\frac{\pi(x-iy)}{b}} - e^{\frac{-id\pi}{b}} \right)} \\
&= \frac{4\pi}{b} \frac{\left(e^{\frac{\pi x}{b}} + e^{\frac{3\pi x}{b}} \right) \cos\left(\frac{\pi y}{b}\right) \sin\left(\frac{d\pi}{b}\right) - e^{\frac{2\pi x}{b}} \sin\left(\frac{2d\pi}{b}\right)}{\left(e^{\frac{\pi(x+iy)}{b}} - e^{\frac{id\pi}{b}} \right) \left(e^{\frac{\pi(x+iy)}{b}} - e^{\frac{-id\pi}{b}} \right) \left(e^{\frac{\pi(x-iy)}{b}} - e^{\frac{id\pi}{b}} \right) \left(e^{\frac{\pi(x-iy)}{b}} - e^{\frac{-id\pi}{b}} \right)}. \tag{82}
\end{aligned}$$

Though it is not done here, we note that we can also use this technique to find an expression for the x -derivative (and thus the electric field).

□

A Extra contour plots

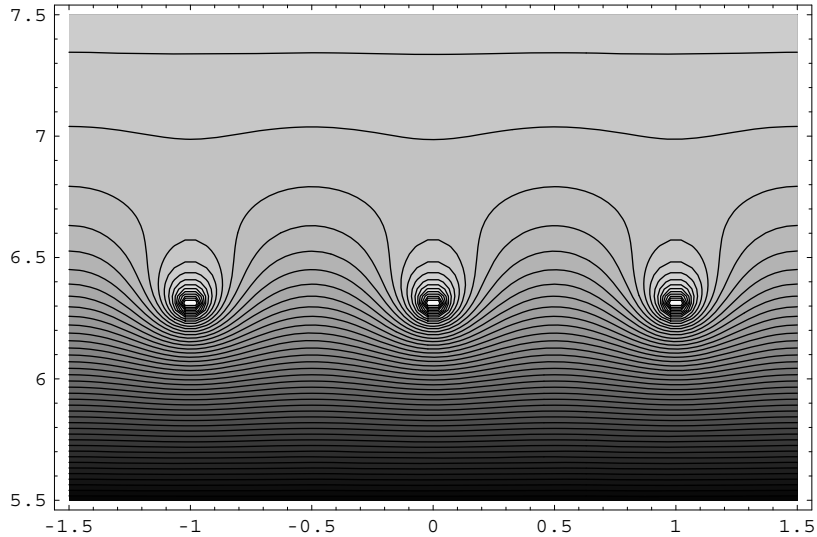


Figure 10: Contour plot of $V(x, y)$ transparent, near grid 2.

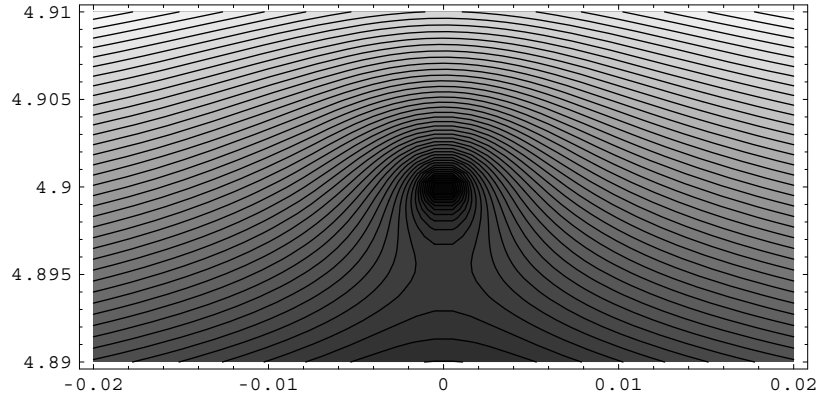


Figure 11: Contour plot of $V(x, y)$ transparent, close-up on grid 1.

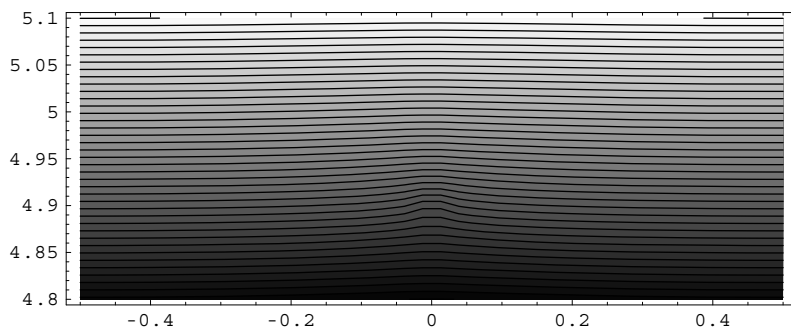


Figure 12: Contour plot of $V(x, y)$ transparent, near grid 1.

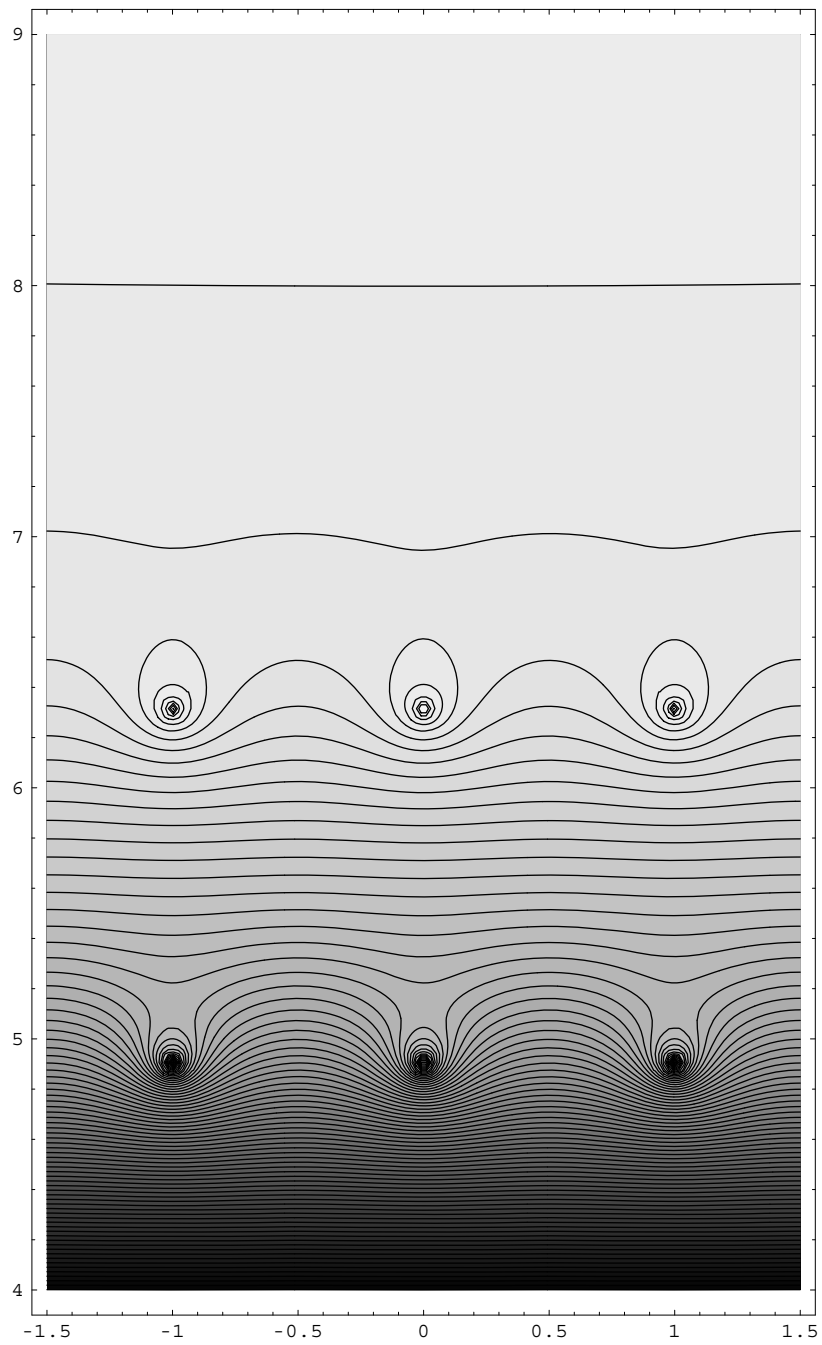


Figure 13: Contour plot of $V(x, y)$ intercepting, near grids 1 and 2.

Acknowledgements

Thanks to Kirk McDonald for posing the intriguing problem of explicitly modelling a wire grid for particle detectors.

References

- [B] Bunemann, O. *et al.*, *Design of Grid Ionization Chambers*, Can. J. Res. (Sec. A) **27**, 191 (1949), http://kirkmcd.princeton.edu/examples/detectors/bunemann_cjr_27_191_49.pdf
- [BR] Blum, W. and Rolandi, L., *Particle Detection With Drift Chambers* (Springer-Verlag, 1993), http://kirkmcd.princeton.edu/examples/detectors/blum_93.pdf
- [M] McDonald, K.T., *Notes on Electrostatics Wire Grids*, (Mar. 5, 2003), <http://kirkmcd.princeton.edu/examples/grids.pdf>
- [SS] Stein, Elias M. and Rami Shakarchi, *Complex Analysis* (Princeton U. 2003).